Deletion of the Brain-Specific α and δ Isoforms of Adapter Protein SH2B1 Protects Mice From Obesity

Jessica L. Cote,[1] Lawrence S. Argetsinger,[2] Anabel Flores,[3] Alan C. Rupp,[4] Joel M. Cline,[2] Lauren C. DeSantis,[2] Alexander H. Bedard,[2] Devika P. Bagchi,[2] Paul B. Vander,[2] Abrielle M. Cacciaglia,[2] Erik S. Clutter,[2] Gowri Chandrashekar,[2] Ormond A. MacDougald,[2,3,4] Martin G. Myers Jr.,[1,2,3,4] and Christin Carter-Su[1,2,3,4]

Diabetes 2021;70:400–414 | https://doi.org/10.2337/db20-0687

Mice lacking SH2B1 and humans with variants of SH2B1 display severe obesity and insulin resistance. SH2B1 is an adapter protein that is recruited to the receptors of multiple hormones and neurotrophic factors. Of the four known alternatively spliced SH2B1 isoforms, SH2B1β and SH2B1γ exhibit ubiquitous expression, whereas SH2B1α and SH2B1δ are essentially restricted to the brain. To understand the roles for SH2B1α and SH2B1δ in energy balance and glucose metabolism, we generated mice lacking these brain-specific isoforms (αδ knockout [αδKO] mice). αδKO mice exhibit decreased food intake, protection from weight gain on standard and high-fat diets, and an adiposity-dependent improvement in glucose homeostasis. SH2B1 has been suggested to impact energy balance via the modulation of leptin action. However, αδKO mice exhibit leptin sensitivity that is similar to that of wild-type mice by multiple measures. Thus, decreasing the abundance of SH2B1α and/or SH2B1δ relative to the other SH2B1 isoforms likely shifts energy balance toward a lean phenotype via a primarily leptin-independent mechanism. Our findings suggest that the different alternatively spliced isoforms of SH2B1 perform different functions in vivo.

Human mutations in *SH2B1* are associated with severe, early-onset obesity, hyperphagia, and often disproportionately high insulin resistance (1–3). Similarly, mice null for *Sh2b1* (*Sh2b1* knockout [KO] mice) exhibit hyperphagic obesity and impaired glucose homeostasis (4,5). Reintroduction of SH2B1β into neurons in *Sh2b1* KO mice largely restores normal body weight and glucose homeostasis (6), suggesting the importance of neuronal SH2B1 for metabolic control. SH2B1 is an adapter protein that regulates responses to multiple hormones and neurotrophic factors that regulate the nervous system. For example, SH2B1 binds to and modulates the activity of the tyrosine kinase JAK2, which forms a complex with several cytokine family receptors including the leptin receptor (LepRb). SH2B1 also binds to and modulates actions of the insulin receptor; TrkA and TrkB, receptors for nerve growth factor (NGF) and brain-derived neurotrophic factor (BDNF), respectively; and RET, a coreceptor for glial cell line–derived neurotrophic factor (GDNF) and growth/differentiation factor-15 (GDF-15) (7,8). When activated, these kinases recruit SH2B1 via its SH2 domain. SH2B1 then facilitates a variety of cellular responses, including changes in the actin cytoskeleton and gene expression (9–11). Consistent with SH2B1's involvement in neurotrophic factor signaling and energy balance and the importance of neurons for appetite control, SH2B1 promotes outgrowth of dendrites and/or axons of cultured primary neurons (12–14) and neurite outgrowth and neuron-specific gene expression in PC12 cells (9,15,16). Hence, SH2B1 influences both structural and functional aspects of the nervous system.

Previous work suggests that SH2B1 contributes to energy balance by modulating LepRb/JAK2 activity (7). Leptin, secreted primarily from white adipose tissue

[1]Neuroscience Program, University of Michigan Medical School, Ann Arbor, MI
[2]Department of Molecular and Integrative Physiology, University of Michigan Medical School, Ann Arbor, MI
[3]Cell and Molecular Biology Program, University of Michigan Medical School, Ann Arbor, MI
[4]Department of Internal Medicine, University of Michigan Medical School, Ann Arbor, MI

Corresponding author: Christin Carter-Su, cartersu@med.umich.edu

Received 30 June 2020 and accepted 12 November 2020

This article contains supplementary material online at https://doi.org/10.2337/figshare.13229090.

(WAT) in approximate proportion to triacylglycerol content, signals the repletion of energy stores to the brain (17). Normal leptin concentrations indicate an adequate fat supply and thus suppress hunger and allow for energy use; conversely, low leptin levels signal low fat stores and thus increase hunger and conserve existing energy stores (17). Consistent with SH2B1 enhancing leptin signaling, *Sh2b1* KO mice exhibit reduced leptin-induced inhibition of food intake and weight gain and dysregulated control of hypothalamic leptin-sensitive gene expression (4,6).

Alternative splicing yields four previously described SH2B1 isoforms—α, β, γ, and δ—which differ only in their COOH-terminal tails (Fig. 1*A* and *B*). In humans, SH2B1β and SH2B1γ are expressed ubiquitously, whereas SH2B1α and SH2B1δ are restricted almost exclusively to the brain (1). In vitro studies indicate that some SH2B1 isoforms possess unique cellular properties. For example, while SH2B1β and SH2B1γ promote neurite outgrowth in PC12 cells (9,15,16), SH2B1α does not, and even inhibits the ability of SH2B1β to do so (2,18). However, before this work, functions of the various SH2B1 isoforms had not been assessed in vivo. Because both SH2B1α and SH2B1δ exhibit the unique characteristic of being expressed almost exclusively in the brain, the central regulator of metabolism, we investigated the combined contributions of these two brain-specific SH2B1 isoforms to energy balance and glucose homeostasis. Our results suggest not only that SH2B1α and/or SH2B1δ are critical regulators of body weight but also that the different alternatively spliced SH2B1 isoforms perform different functions in vivo.

RESEARCH DESIGN AND METHODS

Animal Care

Mice were housed in ventilated cages (~22°C) on a 12-h light/dark cycle (~6:00 AM–6:00 PM) in a pathogen-free animal facility at the University of Michigan. Food and water were available ad libitum except as noted. Experimental mice were fed a standard chow diet (9% fat, cat. no. 5058; LabDiet) or a high-fat diet (HFD) (60% fat, D1249; Research Diets). Experiments were approved by the University of Michigan Institutional Animal Care & Use Committee.

Mouse Model, Genotyping, and Breeding

CRISPR/Cas9 editing was used to delete the regions in *Sh2b1* required for expression of SH2B1α and SH2B1δ ($Sh2b1^{DEL\alpha\delta}$). RNA guides were selected as described previously (19). A 4-kb donor template was designed to juxtapose exon 9 of *Sh2b1*, the sequence in exon 10 that contains the β/γ stop codons, and the region of exon 10 downstream of the α stop codon (Fig. 1*B*). A guide/donor package was injected into C57BL/6J × SJL F2 oocytes, which were implanted into C57BL/6J × SJL F2 mice (University of Michigan Transgenic Animal Model Core). Founders were backcrossed against C57BL/6J mice. See details in Supplementary Material.

Genomic DNA was isolated from tails prior to weaning, and diagnostic fragments were amplified by PCR with Taq polymerase and two primer sets (Supplementary Table 1). Heterozygous $Sh2b1^{DEL\alpha\delta/+}$ (αδHET) mice were backcrossed to C57BL/6J mice for three to five generations. Nonsibling αδHET mice were bred to produce experimental mice. Experimenters were blind to genotypes. Mice were regenotyped after harvest.

Body Weight, Food Intake, Body Composition, and Energy Expenditure

Body weight was assessed weekly. Food intake was monitored once or twice weekly (details in Supplementary Material). Body composition was measured using nuclear magnetic resonance (NMR) (Minispec LF90II; Bruker Scientific). Oxygen consumption (VO_2), carbon dioxide production (VCO_2), and spontaneous locomotor activity were monitored by the Comprehensive Lab Animal Monitoring System (CLAMS) (Columbus Instruments) (Michigan Mouse Metabolic Phenotyping Center) as described previously (3).

Blood Samples

Blood was collected between 9:00 AM and 11:00 AM (glucose, insulin) or 10:00 AM and 2:00 PM (leptin). Glucose levels were measured via tail vein bleeding and Bayer Contour glucometer. Insulin and leptin levels in tail vein blood and terminal trunk blood were measured using Crystal Chem Mouse Insulin ELISA (cat. no. 90080) and Crystal Chem Mouse Leptin ELISA (90030) kits, respectively.

Glucose and Insulin Tolerance Tests

Mice were subjected to a 5- to 6-h morning fast followed by intraperitoneal (i.p.) injection of D-glucose or human insulin. Blood glucose levels were measured as described above.

Leptin Sensitivity

Mice were i.p. injected twice daily (6:00 AM, 6:00 PM) with vehicle (PBS, pH 7.4) (days 1–3, 7–8) or recombinant mouse leptin (days 4–6).

Tissue Harvest and Histology

Mice were anesthetized by isoflurane between 10:00 AM and 2:00 PM and decapitated, and terminal blood was collected. Tissues were dissected, weighed, and fixed in 10% neutral buffered formalin and stored (4°C) for histology or cryopreserved in liquid nitrogen and stored (−80°C) for RNA or protein extraction. Hypothalami (3-mm cubes) were dissected from the ventral diencephalon immediately caudal to the optic chiasm with a coronal brain matrix. Other brain sections were dissected under a dissecting microscope. Fixed liver tissue was paraffin embedded, sectioned (5 μm thickness), stained with hematoxylin-eosin, and imaged, as previously described (20).

RNA Isolation, PCR, and Quantitative PCR

RNA was isolated from frozen tissue with QIAGEN RNeasy Mini Kits (cat. nos. 74104 and 74804). RNA was reverse transcribed into cDNA using TaqMan Reverse Transcription Reagents (Fig. 1*E*) or iScript cDNA Synthesis Kit

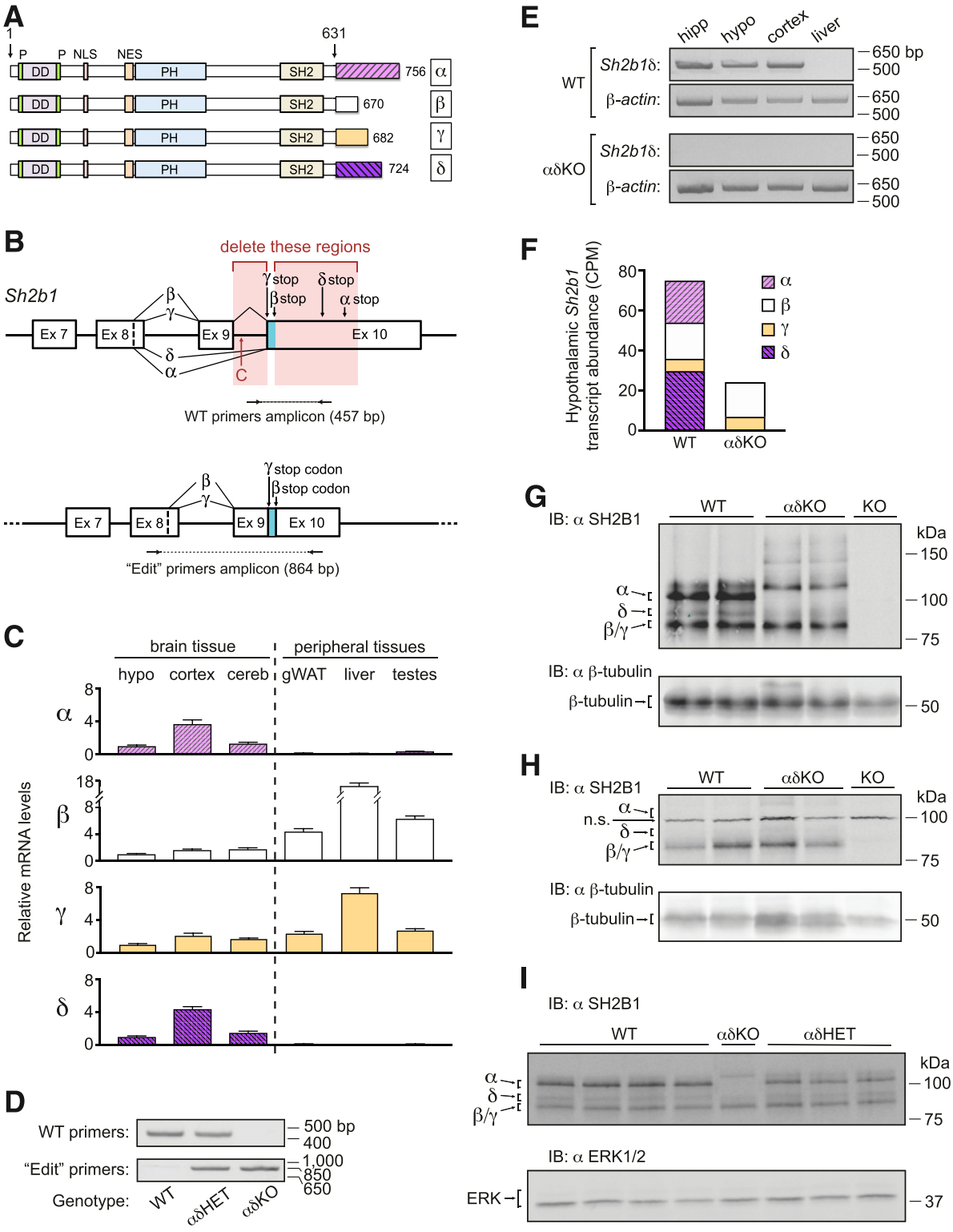

Figure 1—Generation and validation of αδKO mouse model. *A*: Schematic of SH2B1α, SH2B1β, SH2B1γ, and SH2B1δ. Isoform-specific COOH-terminal tails are noted in light purple (diagonally striped), white, yellow, and dark purple (diagonally striped), respectively. Numbers indicate amino acids in mouse and human sequences. P, proline-rich domain; DD, dimerization domain; NLS, nuclear localization sequence; NES, nuclear export sequence; PH, pleckstrin homology domain; SH2, Src homology 2 domain. *B*: Top: Schematic shows strategy to delete the regions of *Sh2b1* that produce the alternative splice variants corresponding to *Sh2b1α* and *Sh2b1δ*. The pink-shaded regions were targeted for deletion, whereas the blue-shaded segment was retained. Stop codons are labeled "stop." Cas9 cut site is indicated by "C." Locations of WT genotyping primers are indicated by horizontal arrows beneath the schematic. Bottom: Schematic depicts donor template for homology-directed repair. Locations of "edit" genotyping primers are indicated by horizontal arrows beneath the schematic. Ex, exon. *C*: RNA was isolated from brain and peripheral tissues of 10- to 12-week-old male WT mice fed standard chow. Transcript levels for *Sh2b1α*, *Sh2b1β*, *Sh2b1γ*, and *Sh2b1δ* were measured by qPCR (n = 4–8 mice/tissue type/isoform). For each isoform, tissue expression levels were

(Figs. 1*C* and 7*A* and Supplementary Fig. 4*A*). Taq polymerase was then used for PCR reactions in Fig. 1*E* (primers listed in Supplementary Table 2). Relative levels of mRNA transcripts encoding SH2B1 isoforms and leptin-regulated genes were determined with TaqMan Gene Expression Assays (details in Supplementary Table 3 and Supplementary Material).

RNA Sequencing

RNA samples had integrity numbers ≥7.5. cDNA library preparation and sequencing were performed by the University of Michigan DNA Sequencing Core. See Supplementary Material for details of preparation and analyses.

Plasmids

cDNAs encoding mouse GFP-SH2B1α (GenBank accession no. AF421138) (18) and rat GFP-SH2B1β (accession no. NM_001048180) (15) have previously been described. cDNA encoding mouse GFP-SH2B18c was created from cDNA encoding mouse GFP-SH2B1γ (accession no. NM_011363.3) (details in Supplementary Material).

PC12 Cell Neurite Outgrowth Assay

PC12 cells (ATCC) were grown and treated and neurite outgrowth experiments were completed as described previously (18) with modifications described in Supplementary Material.

Immunoblotting

Frozen tissues were lysed and homogenized with a glass Dounce homogenizer containing lysis buffer, described previously (3). PC12 cells were transfected and lysed as described previously (18). Equal amounts of protein were immunoblotted with antibody to SH2B1 (cat. no. sc-136065; Santa Cruz Biotechnology), β-tubulin (sc-55529; Santa Cruz Biotechnology), or ERK1/2 (4695S; Cell Signaling Technology) as described previously (3) with modifications in Supplementary Material. Expression levels of SH2B1 isoforms in Fig. 1*I* were quantified using LI-COR Image Studio Lite (version 5.2.5).

Statistics

Statistical analyses of phenotyping data were performed using GraphPad Prism or CalR (21), a custom package of the R programming language designed to analyze indirect calorimetry using ANCOVA. Body weights were compared by two-way repeated-measures ANOVA with Dunnett or Sidak multiple comparisons tests. Cumulative food intake was analyzed by linear regression. See the Supplementary Material for details of statistics used to analyze RNA-seq data. All other comparisons were analyzed by one-way ANOVA with Dunnett multiple comparisons test or two-tailed Student *t* test. $P < 0.05$ was considered significant.

Data and Resource Availability

The data generated during this study are available in the Gene Expression Omnibus repository, GSE145202, or available from the corresponding author upon reasonable request. The mouse model generated during this study is available from the corresponding author upon reasonable request.

RESULTS

Generation of Mice Lacking SH2B1α and SH2B1δ

Exon skipping and an alternative donor site produce four *Sh2b1* splice variants (22,23) (Fig. 1*B*). Consistent with the human tissue expression profile of *SH2B1* mRNA (1), we detected substantial *Sh2b1α* and *Sh2b1δ* mRNA in mouse brain tissue, including hypothalamus, cortex, and cerebellum, but little to none in peripheral tissues including gonadal WAT, liver, and testes; all of these tissues contained *Sh2b1β* and *Sh2b1γ* mRNA (Fig. 1*C*).

To gain insight into the importance of *Sh2b1* splicing in the brain and the contributions of the brain-specific SH2B1α and SH2B1δ isoforms to metabolism in vivo, we used CRISPR/Cas9 to generate mice lacking SH2B1α/δ (Fig. 1*B*). Genotyping (Fig. 1*D*) and DNA sequencing (data not shown) of founder animals and their progeny identified mice containing correctly edited $Sh2b1^{DEL\alpha\delta}$ alleles. αδHET intercrosses produced pups with *Sh2b1* genotypes at the expected Mendelian ratio (data not shown). PCR confirmed that *Sh2b1δ* mRNA transcripts were absent in brain tissue from $Sh2b1^{DEL\alpha\delta/DEL\alpha\delta}$ (αδKO) mice (Fig. 1*E*). Additionally, RNA sequencing (RNA-seq) confirmed the absence of *Sh2b1α/δ* transcripts in αδKO hypothalami and the presence of similar levels of *Sh2b1β/γ* transcripts in $Sh2b1^{+/+}$ (wild type [WT]) and αδKO hypothalami (Fig. 1*F*). We confirmed the absence of SH2B1α/δ proteins, and the continued presence of SH2B1β/γ proteins, in

normalized to expression in the hypothalamus. hypo, hypothalamus; cereb, cerebellum; gWAT, gonadal WAT. *D*: Genomic DNA was purified and analyzed by PCR using WT and "edit" primers. The migration of DNA standards is shown on the right. bp, base pair. *E*: RNA was isolated from brain and liver of WT and αδKO adult male mice and assessed in the same gel for the presence of *Sh2b1δ* or *β-actin* (control). The migration of DNA standards is shown on the right. hipp, hippocampus. *F*: RNA was isolated from hypothalami of 10- to 12-week-old male mice and analyzed by RNA-seq. Transcript abundance of *Sh2b1α*, *Sh2b1β*, *Sh2b1γ*, and *Sh2b1δ* was predicted by StringTie analysis using both annotated and previously unannotated transcripts (*n*: WT = 9, αδKO = 12). CPM, counts per million. Proteins in whole brain (*G*) and liver (*H*) tissue lysates from WT, αδKO, and *Sh2b1* KO adult male mice were immunoblotted with antibody to SH2B1 (α SH2B1) or to β-tubulin (α β-tubulin). The migration of molecular weight standards is shown on the right. The expected migration of the different isoforms (and in *H*, a nonspecific band) is indicated on the left. *I*: Proteins in whole brain lysates from WT, αδKO, and αδHET 10- to 12-week-old female mice were immunoblotted with antibody to SH2B1 or to ERK1/2 (α ERK1/2). The migration of molecular weight standards is shown on the right. The expected migration of the different isoforms is indicated on the left. IB, immunoblot; n.s., nonspecific band. Data are means ± SEM.

αδKO brain lysates (Fig. 1*G*). As expected, only β/γ isoforms were detected in liver tissue from WT and αδKO mice (Fig. 1*H*). SH2B1β/γ protein levels were similar between WT and αδKO mice in liver tissue (Fig. 1*H*) and between WT, αδKO, and αδHET mice in brain tissue (Fig. 1*G* and *I*), whereas SH2B1α/δ protein levels were decreased by ∼40% in αδHET compared with WT brain lysates (Fig. 1*I*). Thus, αδKO mice exhibit the predicted isoform-specific ablation of SH2B1α/δ, and αδHET mice exhibit reduced SH2B1α/δ, without compensatory alterations in expression of SH2B1β/γ isoforms.

Reduced SH2B1α and SH2B1δ Decreases Body Weight and Adiposity in Mice

To determine whether SH2B1α/δ influence energy balance, we fed male and female αδKO, αδHET, and WT littermates standard chow and measured their body weight weekly. Both male and female αδKO mice appeared thinner and weighed considerably less than WT littermates by 8 weeks of age (males) (Fig. 2*A* and *B*) or 20 weeks of age (females) (Supplementary Fig. 1*A*). Body weight of male and female αδHET mice did not diverge from that of controls before 25 weeks; however, the weight of αδHET males was significantly decreased compared with controls at 38–42 weeks (Fig. 2*C* and Supplementary Fig. 1*B*).

While αδKO males exhibited slightly decreased body length and lean mass, these measures were not different from those of sex-matched WT littermates for αδKO females or αδHET mice of either sex (Fig. 2*D* and *E* and Supplementary Fig. 1*C* and *D*), suggesting that differences in overall body size were unlikely to have mediated the decreased body weight of αδKO mice. Indeed, compared to controls, fat mass was decreased in male and female αδKO and male αδHET mice (Fig. 2*F* and Supplementary Fig. 1*E*). Additionally, percent lean mass was increased and percent fat was decreased in αδKO mice of both sexes (Fig. 2*G* and *H* and Supplementary Fig. 1*F* and *G*). Similarly, leptin concentrations and adipose tissue weights were decreased in αδKO mice of both sexes (Fig. 2*I* and *J* and Supplementary Fig. 1*H* and *I*). Thus, while body length was slightly decreased in αδKO males compared with controls, the major effect across sexes was of decreased adiposity in αδKO mice. αδKO liver weight was also decreased compared with controls, which may reflect a decrease in triacylglycerol content (as for animals on HFD [see below]) because the mass of other tissues (e.g., brain) was unchanged (Fig. 2*J* and Supplementary Fig. 1*I*). Furthermore, the decreased body weight and fat mass of αδHET males compared with controls suggest that reduced expression of SH2B1α/δ associated with haploinsufficiency of SH2B1α/δ in males is sufficient to impact body weight and adiposity.

αδKO Mice Exhibit Reduced Food Intake but Normal Energy Expenditure

To determine whether the decreased body weight of αδKO mice resulted from reduced caloric intake, increased energy expenditure, or both, we measured weekly food intake of αδKO and WT littermates when their body weights were diverging. Male (Fig. 3*A* and *B*) and female (Supplementary Fig. 2*A*) αδKO mice consumed less food than controls. We observed no statistically significant alteration in food intake in αδHET versus control mice, consistent with the minor alteration in their body weight. Metabolic cages revealed no differences by genotype in VO_2, respiratory exchange ratio (RER), or locomotor activity (Fig. 3*C*–*F* and Supplementary Fig. 2*B*–*E*). There were also no differences by genotype in VO_2, VCO_2, or energy expenditure when body weight, lean mass, or fat mass were taken into account as covariates in the ANCOVA. These data suggest that the decreased weight of chow-fed αδKO mice results primarily from decreased caloric intake.

Protection From Diet-Induced Obesity in αδKO Mice

To determine whether removal of SH2B1α/δ affords protection from diet-induced obesity (DIO), we challenged αδKO and WT littermates with an HFD. Males were used because of their enhanced susceptibility to DIO relative to females (24,25). HFD-fed αδKO mice gained significantly less weight than controls (Fig. 4*A*). In fact, their body weight remained near to or below that of chow-fed WT mice for the entire study (compare with Fig. 2*A*). HFD-fed αδKO mice consumed amounts of food similar to those of controls (Fig. 4*B* and *C*). The finding that the body weight of HFD-fed αδKO mice was reduced but their food intake was normal suggests that they expended more energy than controls. Body composition measurements revealed that, as for chow-fed mice, the decreased body weight of HFD-fed αδKO mice resulted primarily from decreased fat mass (Fig. 4*D*–*G*). While leptin levels were highly variable and not significantly different by genotype, they trended lower in αδKO mice (Fig. 4*H*). Similar to chow-fed animals, HFD-fed αδKO mice exhibited reduced weight of inguinal WAT and liver (Fig. 4*I*). Histological analysis of liver tissue detected less lipid in livers of HFD-fed αδKO mice compared with controls, suggesting that decreased steatosis may underlie the lower weight of αδKO livers (Fig. 4*J*).

Adiposity-Dependent Improvements in Glucose Metabolism in αδKO Mice

To determine whether deletion of SH2B1α/δ impacts glucose metabolism, we first measured glucose and insulin in ad libitum–fed or overnight-fasted αδKO and WT mice (22–27 weeks old). Fed αδKO males displayed normal blood glucose levels but low insulin concentrations (Fig. 5*A* and *B*). When fasted, αδKO males exhibited low blood glucose and insulin concentrations (Fig. 5*C* and *D*). Glucose and insulin tolerance tests revealed improved glucose tolerance in 28- to 32-week-old chow-fed αδKO males (Fig. 5*E* and *F*) and improved glucose tolerance and insulin sensitivity in 18- to 20-week-old HFD-fed αδKO males (Fig. 5*G* and *H*). In chow-fed αδKO females, parameters of glucose metabolism were unchanged except that their insulin concentrations were decreased in the fed state (Supplementary Fig. 3*A*–*F*). Thus, αδKO mice generally

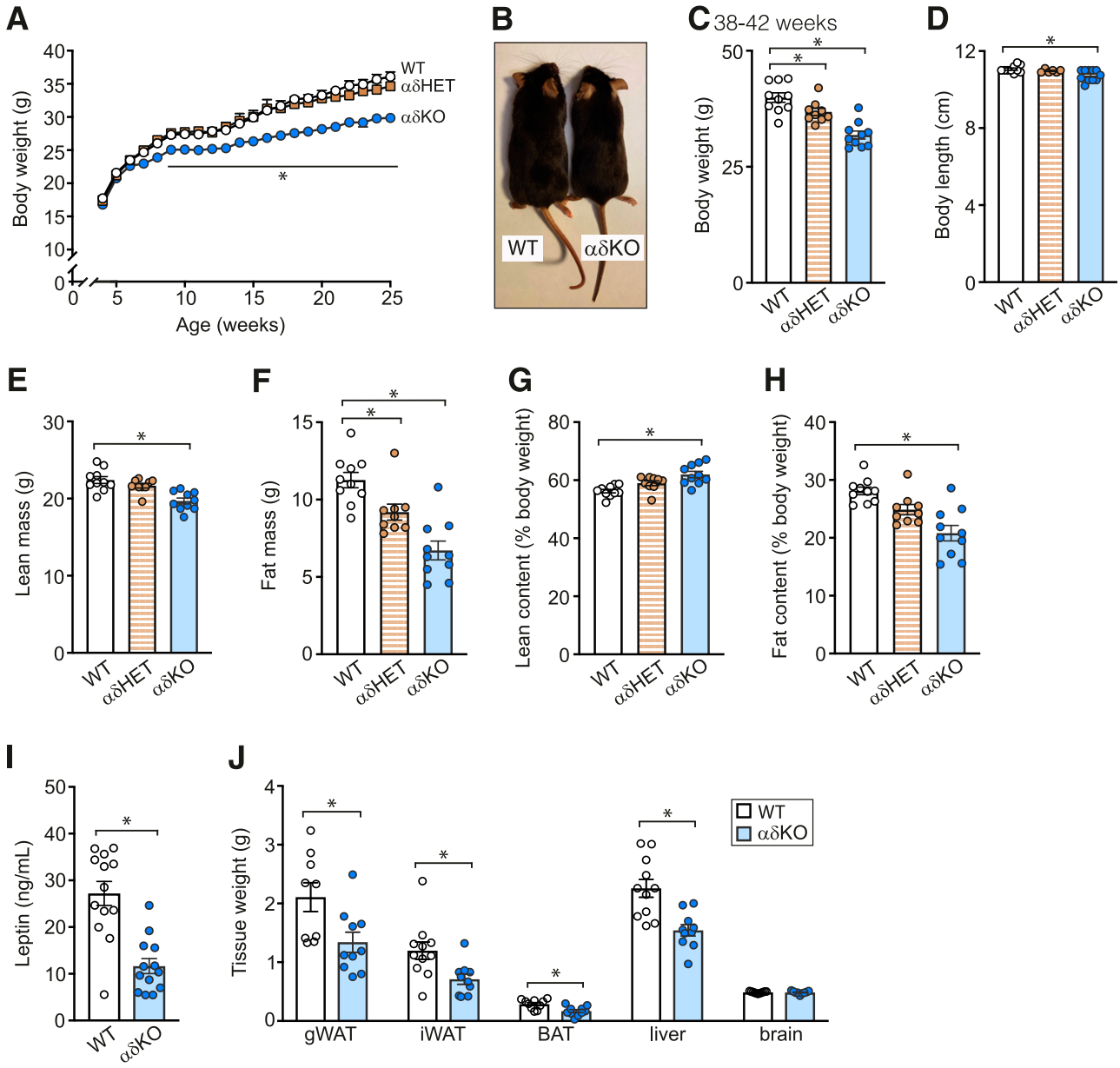

Figure 2— Male αδKO mice fed standard chow exhibit reduced body weight, fat content, circulating leptin levels, adipose tissue weight, and liver weight. *A*: Body weight was measured weekly from 4 to 25 weeks (*n*: WT = 9–13, αδHET = 8–11, αδKO = 6–10). *B*: Representative 36-week-old WT and αδKO mice. *C*: Body weight was measured between 38 and 42 weeks of age (*n*: WT = 10, αδHET = 9, αδKO = 10). *D*: Body length was measured from nose to anus in 38- to 42-week-old mice (*n*: WT = 10, αδHET = 6, αδKO = 11). *E–H*: Body composition of 38- to 42-week-old mice was analyzed by NMR between 9:00 AM and 11:00 AM (*n*: WT = 10, αδHET = 9, αδKO = 10). *I*: Blood was collected from 38- to 42-week-old mice fed ad libitum, and serum leptin levels were measured by ELISA (*n*: WT = 13, αδKO = 13). *J*: Tissues of 38- to 42-week-old mice were dissected and weighed (*n*: WT = 9–11, αδKO = 10). BAT, brown adipose tissue; gWAT, gonadal WAT; iWAT, inguinal WAT. See Supplementary Fig. 1 for corresponding data from female mice. Statistics: two-way repeated-measures ANOVA (weeks 7–25) (*A*), one-way ANOVA (*C–H*), and unpaired, two-tailed Student *t* test (*I* and *J*). *$P < 0.05$. Data are means ± SEM.

exhibit improved glucose tolerance and insulin responsiveness compared with their more obese littermate controls. Together with the improved glucose homeostasis in the lean αδKO males, the relatively normal glucose metabolism in αδKO females, which exhibit a more modest reduction in body weight, suggested that alterations in glucose homeostasis in αδKO mice might result not directly from the lack of SH2B1α/δ but, rather, from decreased adiposity. We therefore assessed glucose homeostasis in young, 10- to 12-week-old chow-fed male αδKO mice, when their fat content was similar to that of controls (Fig. 6*A*). Their decreased leptin levels (Fig. 6*B*) suggested that some differences in adiposity were beginning to develop. We observed no differences by genotype in glucose or insulin concentrations, glucose tolerance, or insulin sensitivity in these young animals (Fig. 6*C–H*). Thus,

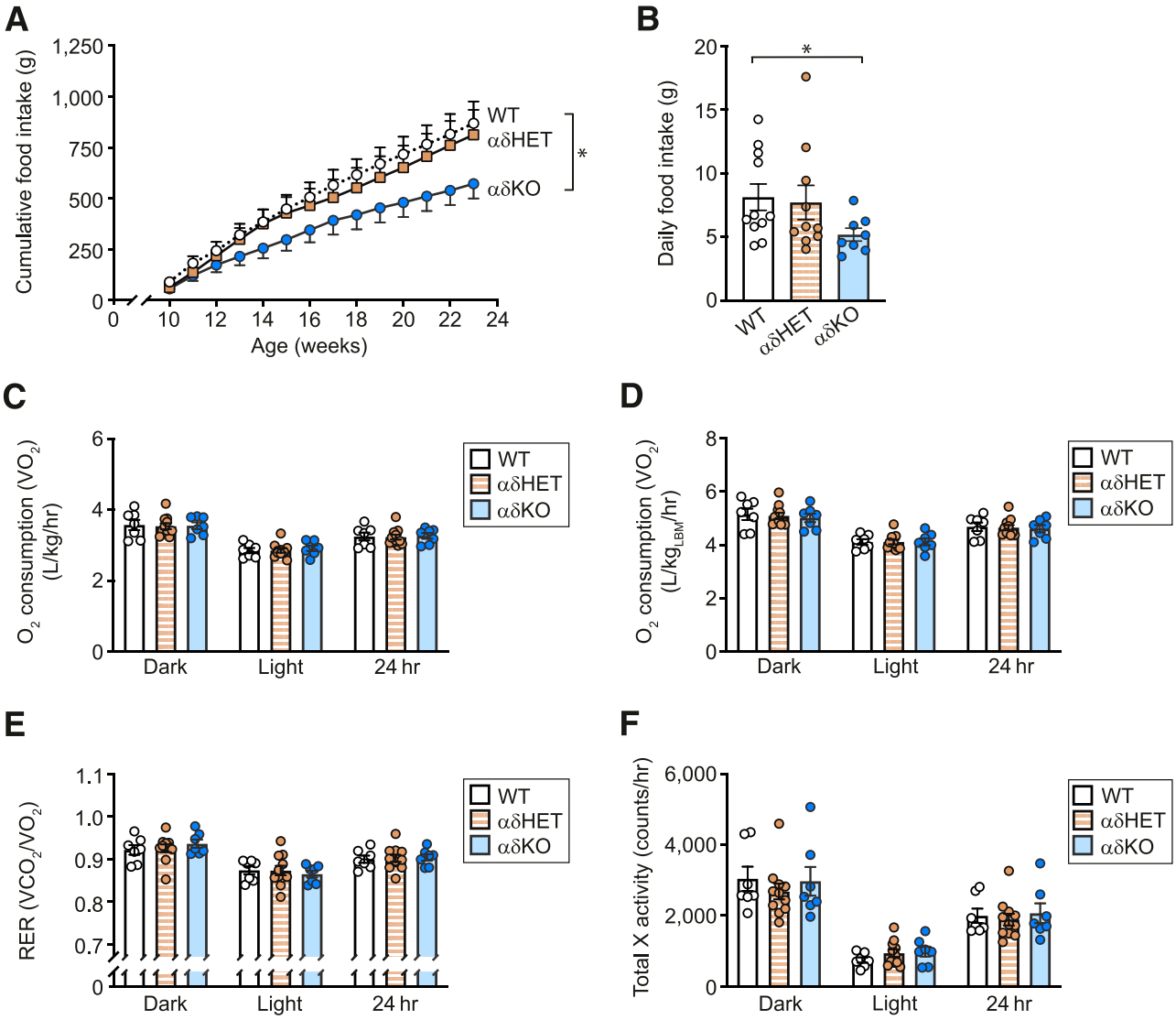

Figure 3—Male αδKO mice fed standard chow exhibit decreased food consumption but normal energy expenditure. *A*: Food intake was measured weekly from 10 to 23 weeks (*n*: WT = 11, αδHET = 10, αδKO = 8). *B*: Average daily food intake during final 10 weeks of measurements shown in *A* (*n*: WT = 11, αδHET = 10, αδKO = 8). *C–F*: Energy expenditure was measured in 10- to 12-week-old mice by CLAMS (*n*: WT = 7, αδHET = 11, αδKO = 7). Parameters included VO_2 corrected for total body weight (*C*) or lean body mass (LBM) (*D*), RER (*E*), and total motor activity in the X dimension (*F*). RER was calculated as VCO_2/VO_2. The final 24 h of recordings are presented. See Supplementary Fig. 2 for corresponding data from female mice. Statistics: linear regression analysis (weeks 10–23) (*A*) and one-way ANOVA (*B–F*). *$P < 0.05$. Data are means ± SEM. hr, hour.

the improved glucose homeostasis observed in older αδKO mice is likely to be secondary to their reduced adiposity rather than the result of any direct effect of removal of SH2B1α/δ.

Normal Leptin Sensitivity in αδKO Mice

Because SH2B1 modulates leptin signaling and SH2B1α/δ expression is restricted to the brain, the site of leptin action on food intake and energy balance, we examined the possibility that increased leptin signaling might underlie the leanness of αδKO mice. The arcuate nucleus of the hypothalamus is a primary target for leptin (26,27). Leptin action in the arcuate nucleus inhibits the expression of appetite-stimulating neuropeptides agouti-related peptide (AgRP) and neuropeptide Y (NPY) and promotes the expression of appetite-suppressing neuropeptides pro-opiomelanocortin (POMC) and cocaine- and amphetamine-regulated transcript (CART) (28). Leptin also regulates the expression of other genes in LepRb-expressing cells in the hypothalamus (29). We measured expression of eight relevant leptin-regulated, protein-encoding genes (*Agrp*, *Npy*, *Pomc*, *Cartpt*, *Asb4*, *Irf9*, *Ghrh*, *Serpina3n*) in αδKO and WT hypothalami using quantitative PCR (qPCR). To avoid potential confounding by differences in adiposity and/or circulating leptin levels, which would impact leptin action, we assessed young, 10- to 12-week-old male mice. We

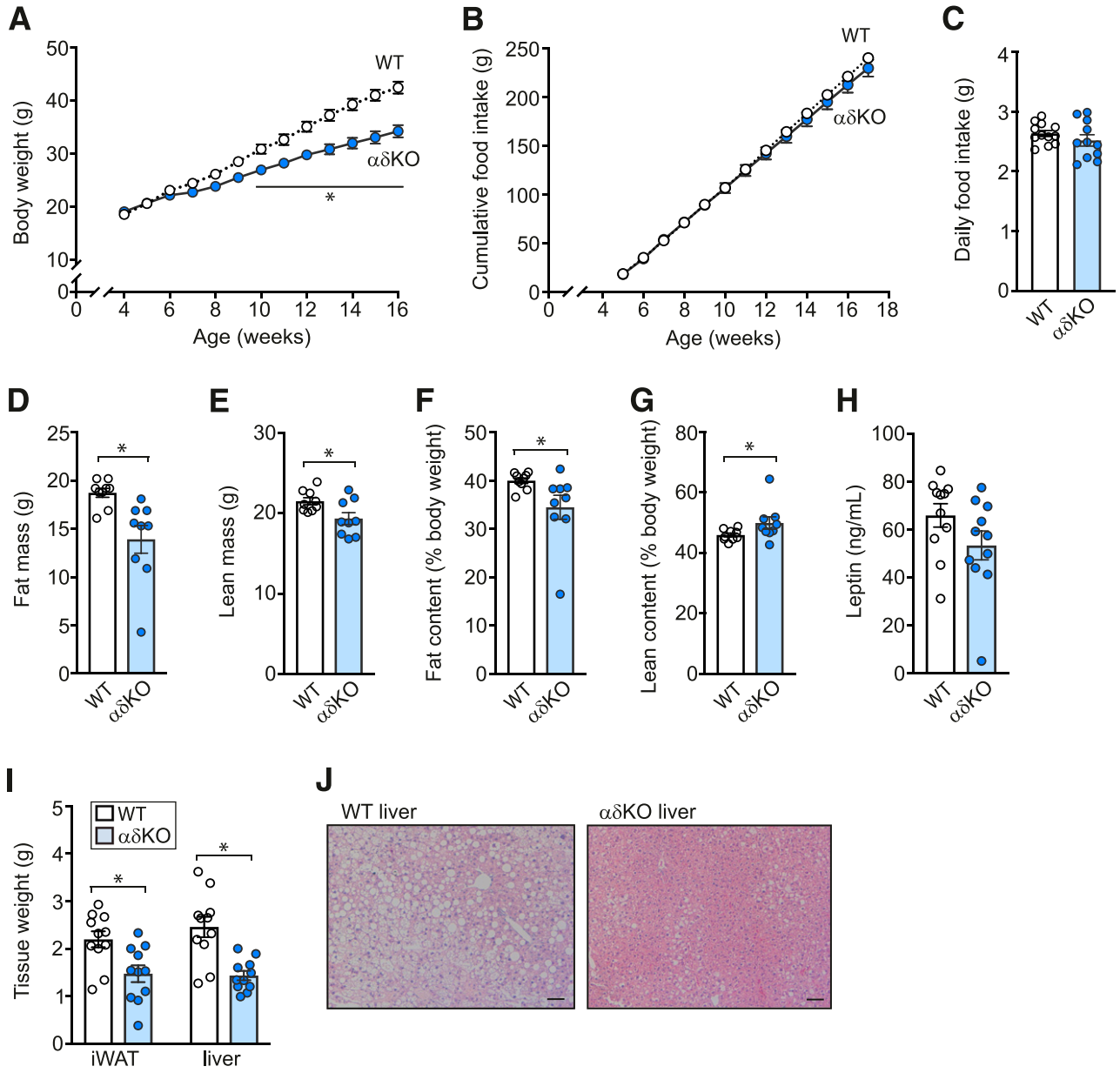

Figure 4—αδKO mice are protected against DIO. *A*: Body weight was measured weekly from 4 to 16 weeks (*n*: WT = 12–13, αδKO = 11–12). *B*: Cumulative food intake was measured twice weekly from 5 to 17 weeks (*n*: WT = 12, αδKO = 11). *C*: Average daily food intake during the 12 weeks of measurements shown in *B* (*n*: WT = 12, αδKO = 11). *D*–*G*: Body composition was analyzed in 21- to 23-week-old mice by NMR between 9:00 AM and 11:00 AM (*n*: WT = 9, αδKO = 9). *H*: Blood was collected from 21- to 23-week-old mice fed ad libitum, and serum leptin levels were measured by ELISA (*n*: WT = 11, αδKO = 11). *I*: Tissues of 21- to 23-week-old mice were dissected and weighed (*n*: WT = 11, αδKO = 11). iWAT, inguinal WAT. *J*: Liver tissues from 21- to 23-week-old mice were paraffin embedded and stained with hematoxylin-eosin. Images are representative of indicated genotypes (*n*, livers imaged: WT = 3, αδKO = 5). Scale bar, 50 μm. Statistics: two-way repeated-measures ANOVA (weeks 4–16) (*A*), linear regression analysis (weeks 5–17) (*B*), and unpaired, two-tailed Student *t* test (*C*–*I*). *$P < 0.05$. Data are means ± SEM.

found no differences by genotype in expression of these genes (Fig. 7*A*).

To more directly test the effects of SH2B1α/δ on leptin sensitivity, we examined the responses of 6-week-old αδKO and WT mice to low-dose leptin injections. We have previously used this assay to identify increased leptin sensitivity in other mouse lines (3,30,31). At this age, there was no difference in circulating leptin levels between αδKO and WT littermates (Fig. 7*B*). We observed no difference by genotype in rate of weight loss or food intake reduction (Fig. 7*C* and *D*) in response to leptin treatment. In conjunction with the WT-like expression levels of leptin-responsive genes in αδKO hypothalami, these results suggest that removal of SH2B1α/δ does not alter leptin

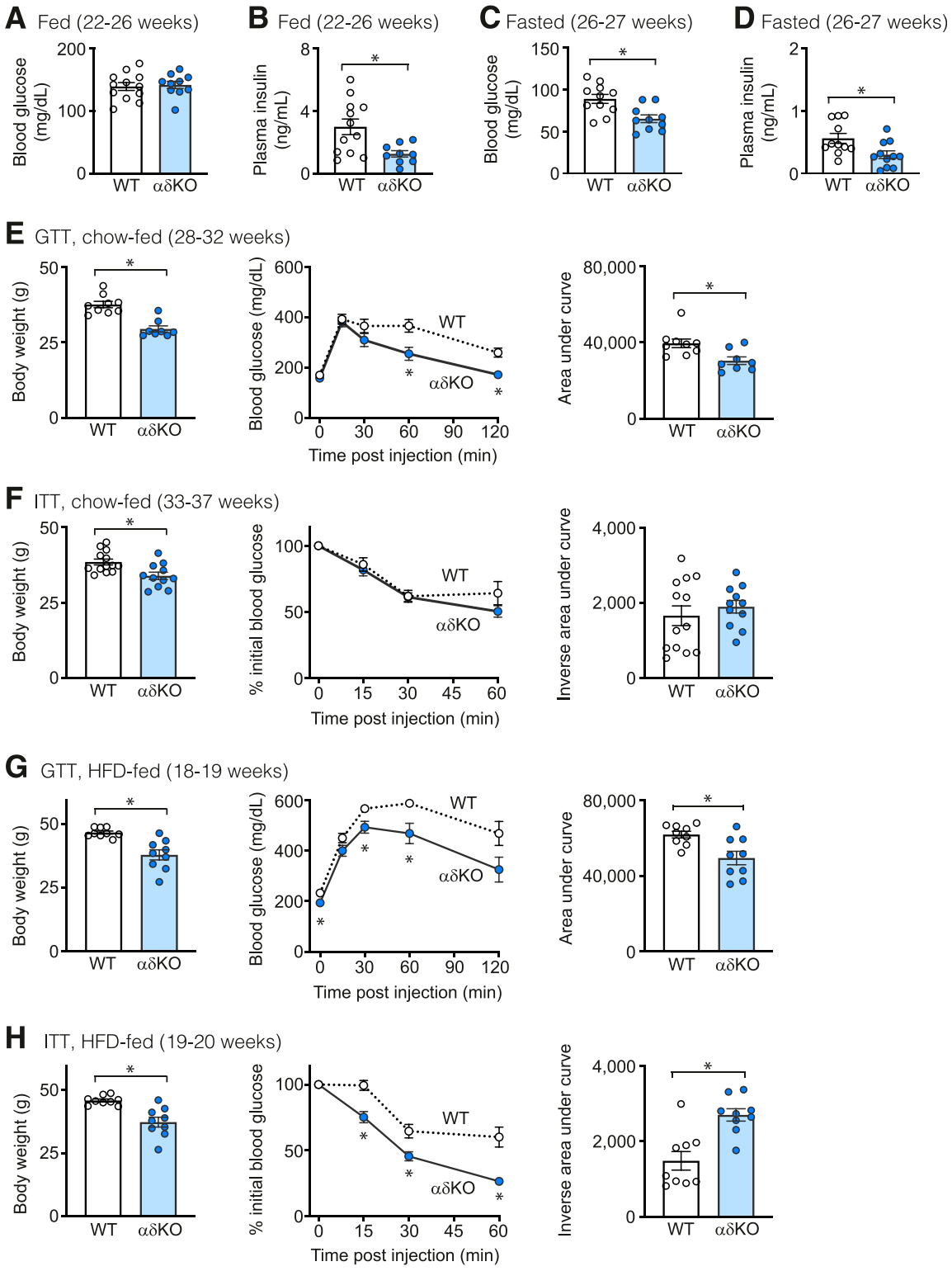

Figure 5—Older male αδKO mice exhibit improved glucose homeostasis. Blood was collected from 22- to 26-week-old mice fed chow ad libitum, and blood glucose levels were measured by glucometer (*n*: WT = 12, αδKO = 10) (*A*) and plasma insulin levels were measured by ELISA (*n*: WT = 12, αδKO = 9) (*B*). Blood was collected from 26- to 27-week-old chow-fed mice fasted overnight (16 h), and blood glucose levels were measured by glucometer (*n*: WT = 11, αδKO = 10) (*C*) and plasma insulin levels were measured by ELISA (*n*: WT = 11, αδKO = 11) (*D*). *E*: Glucose tolerance tests (GTTs) were performed on 28- to 32-week-old chow-fed mice following i.p. injection with glucose (2 g/kg) (*n*: WT = 9, αδKO = 8). Area under the curve for each animal was calculated using a baseline of $y = 0$. *F*: Insulin tolerance tests (ITTs) were performed on 33- to 37-week-old chow-fed mice following i.p. injection with insulin (1 unit/kg) (*n*: WT = 13, αδKO = 11). Data are reported as % initial blood glucose values. Inverse area under the curve for each animal was calculated using a baseline of $y = 100$. *G*: GTTs were performed on 18- to 19-week-old HFD-fed mice following i.p. injection with glucose (2 g/kg) (*n*: WT = 9, αδKO = 9). Area under the curve for

action but, rather, protects mice from obesity primarily via leptin-independent mechanisms.

Altered Transcriptome in αδKO Hypothalami

To gain additional insight into mechanisms underlying the leanness of αδKO mice, we examined the impact of deleting SH2B1α/δ on hypothalamic gene expression using RNA-seq. Given that WT and αδKO mice had similar fat content at the time of hypothalamic dissection (Fig. 6*A*), changes in gene expression were expected to be adiposity independent. The combined expression of all *Sh2b1* transcripts annotated in the Ensembl mouse genome was substantially decreased in αδKO mice, as predicted (Supplementary Fig. 5*B*). RNA-seq identified 59 additional genes that exhibited statistically significant differential regulation by genotype. Of these, 29 were upregulated and 30 were downregulated in αδKO mice (Fig. 8*A* and Supplementary Tables 4 and 5). qPCR analysis validated the gene expression changes of a representative sample (*Slc5a11*, *C1qa*, *Gsg1l*, *Kdm8*) of the up- and downregulated genes identified by RNA-seq (Supplementary Fig. 4*A*). We compared the hypothalamic transcriptional changes that we observed in αδKO mice with published results from leptin-treated mice (29). There was no correlation between data sets among all genes that were differentially expressed or among the genes that were statistically significantly regulated (Fig. 8*B* and *C*). These results provide further evidence that removal of SH2B1α/δ protects mice from obesity via leptin-independent mechanisms.

Interestingly, Gene Ontology (GO) revealed that changes in the transcriptional profile of hypothalamic tissue from αδKO mice were significantly associated with several genes linked to microglial function (Supplementary Fig. 4*B*). Similarly, querying MouseMine revealed that many of the mouse phenotypes that significantly associate with differentially expressed genes in αδKO mice were related to microglia (Supplementary Fig. 4*C*). Also, comparison with a previously published mouse hypothalamic single-cell RNA-seq data set that contained expression profiles for all hypothalamic cell types including neurons, microglia, and macrophages (32) indicated that most of the genes with statistically significant differential regulation in αδKO hypothalami were predominantly expressed in microglia and/or macrophages (Supplementary Fig. 4*D*). In addition, *Sh2b1* was expressed in all hypothalamic cell types including neurons, microglia, and macrophages (32). These findings provide evidence that deletion of SH2B1α/δ impacts hypothalamic microglial function. Interestingly, most of the microglia-related genes (*C1qa*, *C1qb*, *Cx3cr1*, *Grn*, *Trem2*, *Tyrobp*) that exhibited statistically significantly upregulated expression in our data set have previously been identified as contributors to complement-mediated synaptic pruning (33–37), presenting the possibility that SH2B1α/δ may regulate structural changes at synapses. The ability of SH2B1α/δ to regulate structural changes at synapses would be consistent with previous in vitro findings that SH2B1 regulates the actin cytoskeleton (10,11,14).

Novel *Sh2b1* Transcripts May Exist

A byproduct of our RNA-seq analysis was greater insight into *Sh2b1* transcripts. Our initial quantification of *Sh2b1* transcripts using StringTie included only transcripts that had previously been annotated in the Ensembl mouse genome (Supplementary Fig. 5*A*). However, this analysis suggested that almost no mRNA encoding SH2B1α was detected in WT hypothalami (Supplementary Fig. 5*B*), which contradicted our qPCR data (Fig. 1*C*). We reanalyzed the data to include previously unannotated transcripts. This analysis revealed six potential novel *Sh2b1* transcripts in WT mice (Supplementary Fig. 5*A*). Inclusion of unannotated alongside annotated transcripts provided a more accurate measurement of *Sh2b1* transcript abundance (Supplementary Fig. 5*C*). This revised sum of RNA-seq transcripts more closely matches total *Sh2b1* gene expression measured by qPCR (Supplementary Fig. 5*D*).

While four of six potential novel (unannotated) *Sh2b1* transcripts are slight variations of known transcripts, the remaining two differ notably from known transcripts in that their eighth intron is not spliced out (Supplementary Figs. 5*A* and 6). We named these predicted transcripts "*Sh2b18c*" for their unique eighth exon.

Sh2b18c mRNA contains an in-frame stop codon located 263 base pairs downstream of exon 8 and is predicted to be targeted for nonsense-mediated decay (38). Regardless, to examine potential expression of *Sh2b18c*-encoded proteins, we generated a GFP-SH2B18c expression vector and transfected it into PC12 cells. GFP-SH2B18c migrated at its predicted molecular size on SDS-PAGE gels (Supplementary Fig. 5*E*) and enhanced neurite outgrowth to an extent similar to that of SH2B1β (Supplementary Fig. 5*F*), suggesting that if it were expressed, it might function similarly to SH2B1β or SH2B1γ. However, αδKO brain lysates showed no increase in SH2B1 protein migrating at the expected size of SH2B18c on SDS-PAGE gels (Supplementary Fig. 5*E*), despite the increased *Sh2b18c* mRNA in these mice. Thus, when combined with our prediction that the *Sh2b18c* transcripts would be targeted for nonsense-mediated decay, this lack of an appropriately migrating band makes it unlikely that *Sh2b18c* transcripts contributed to the αδKO phenotype.

each animal was calculated using a baseline of $y = 0$. *H*: ITTs were performed on 19- to 20-week-old HFD-fed mice following i.p. injection with insulin (1 unit/kg) (*n*: WT = 9, αδKO = 9). Data are reported as % initial blood glucose values. Inverse area under the curve for each animal was calculated using a baseline of $y = 100$. *E–H*: Body weights corresponding to each experiment are shown. See Supplementary Fig. 3 for corresponding data from females. Statistics: unpaired, two-tailed Student *t* test (*A–H*). $^*P < 0.05$. Data are means ± SEM.

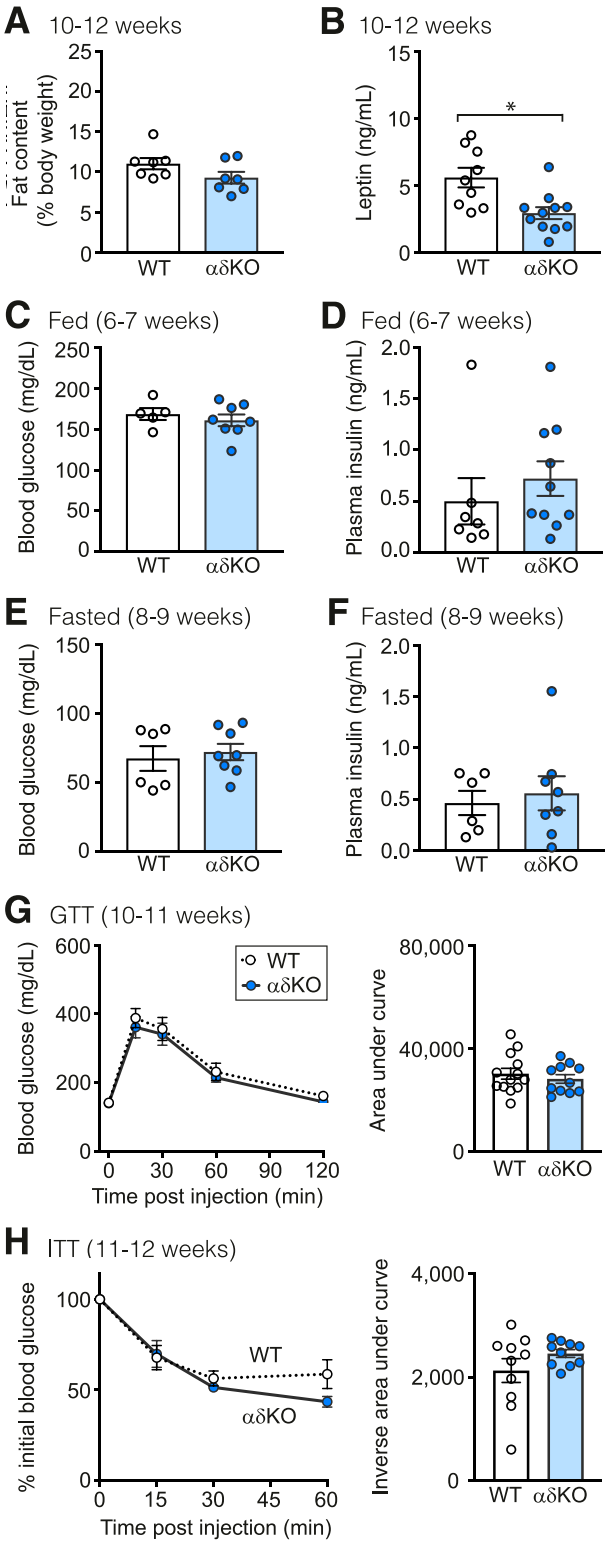

Figure 6—Young male αδKO mice (6–12 weeks old) exhibit normal glucose homeostasis. *A*: Fat content was analyzed by NMR in 10- to 12-week-old mice (*n*: WT = 7, αδKO = 7). *B*: Blood was collected from 10- to 12-week-old mice fed ad libitum, and serum leptin levels were measured by ELISA (*n*: WT = 9, αδKO = 11). Blood was collected from 6- to 7-week-old mice fed ad libitum, and blood glucose levels were measured by glucometer (*n*: WT = 5, αδKO = 8) (*C*) and plasma insulin levels were measured by ELISA (*n*: WT = 7, αδKO = 10) (*D*). Blood was collected from 8- to 9-week-old mice fasted overnight (16 h), and blood glucose levels were measured by glucometer (*n*: WT = 6, αδKO = 8) (*E*) and plasma insulin levels were measured by ELISA (*n*: WT = 6, αδKO = 8) (*F*). *G*: Glucose tolerance tests (GTTs) were performed on 10- to 11-week-old mice following i.p. injection with glucose (2 g/kg) (*n*: WT = 13, αδKO = 11). Area under the curve for each animal was calculated using a baseline of $y = 0$. *H*: Insulin tolerance tests (ITTs) were performed on 11- to 12-week-old mice following i.p. injection with insulin (1 unit/kg) (*n*: WT = 10, αδKO = 10). Data are reported as % initial blood glucose values. Inverse area under the curve for each animal was calculated using a baseline of $y = 100$. Statistics: unpaired, two-tailed Students *t* test (*A–H*). *$P < 0.05$. Data are means ± SEM.

DISCUSSION

Here we create a novel mouse model that lacks two isoforms of adapter protein SH2B1, α and δ, both of which are expressed almost exclusively in brain tissue. We demonstrate that αδKO mice gain less weight than controls and are protected against DIO. The decreased body weight of the chow-fed αδKO mice results primarily from suppressed food intake. Additionally, the αδKO mice exhibit adiposity-dependent improvements in glucose homeostasis. Thus, SH2B1α and/or SH2B1δ are critical determinants of energy balance and, indirectly, glucose homeostasis.

Most isoform-specific KO models exhibit phenotypes that are similar to, yet less severe than, those of animals with the complete KO (39). Thus, given the obesity of *Sh2b1* KO mice, the simplest prediction for mice lacking two of four known SH2B1 isoforms would be an overweight phenotype. However, αδKO mice, lacking two of four known SH2B1 isoforms, and approximately half the normal SH2B1 brain protein content, are underweight. These findings suggest that the different SH2B1 isoforms make nonredundant, even opposing, contributions to the regulation of energy balance. Furthermore, normal expression of SH2B1β/γ is not sufficient to maintain normal energy balance, suggesting that the ratio of SH2B1 isoforms must be carefully titrated for the body to appropriately balance its energy. We investigated whether altering the ratio of the isoforms could be a defense against famine or overeating. However, preliminary studies indicated that the ratios of the various isoforms do not appear to be regulated by a 24-h fast or an HFD (data not shown). Nevertheless, our finding that in the brain WT mice have a high ratio of SH2B1α/δ to SH2B1β/γ protein levels, αδHET mice have a medium ratio, and αδKO mice have a ratio of zero suggests that the lower the ratio of SH2B1α/δ to SH2B1β/γ, the stronger the resistance to weight gain. Therefore, we propose that manipulating the ratio of SH2B1 isoforms, perhaps by identifying molecular targets that could be modified to alter *SH2B1* splicing activity or disrupt the expression of SH2B1α/δ specifically, may serve as the basis for new obesity therapeutics. It is also possible that other physiological stressors and/or genetic variants or mutations may impact the SH2B1 isoform ratio and, as a consequence, energy balance.

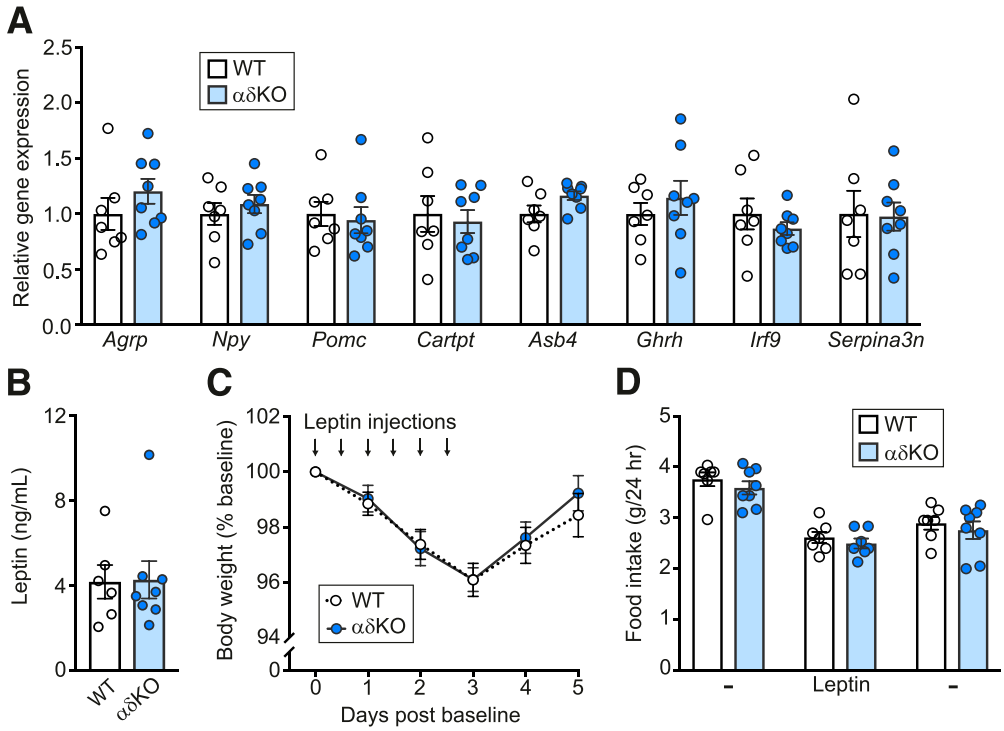

Figure 7—αδKO mice exhibit normal expression levels of leptin-regulated genes in the hypothalamus and normal sensitivity to exogenous leptin. *A*: RNA was isolated from hypothalami of 10- to 12-week-old male mice. Expression levels of leptin-responsive genes were measured by qPCR (*n*: WT = 7, αδKO = 8). αδKO results were normalized to the average relative expression obtained for WT samples. *B*: Blood was collected from 6-week-old male mice fed ad libitum, and plasma leptin levels were measured by ELISA (*n*: WT = 6, αδKO = 8). Body weight (*C*) and food intake (*D*) were measured before, during, and after i.p. injections of vehicle (−) or leptin (1 mg/kg) in 6-week-old mice (*n*: WT = 7, αδKO = 8). Average values from days 1–3 served as baseline. Statistics: no significant differences by unpaired, two-tailed Student *t* test (*A*–*D*). Data are means ± SEM. hr, hour.

The lean phenotype of αδKO mice is consistent with known cellular actions of the individual SH2B1 isoforms. Specifically, in PC12 cells, SH2B1α was shown to inhibit SH2B1β enhancement of NGF-induced neurite outgrowth by a process that appears to be dependent on NGF-induced phosphorylation of a specific tyrosine unique to the COOH terminus of SH2B1α (18). Thus, the simplest explanation of the αδKO phenotype is that in these mice, removal of SH2B1α enhances the activity of SH2B1β, and presumably SH2B1γ, to enhance the actions of neurotrophic factor receptors known to recruit SH2B1 isoforms. One can envision that the competing actions of SH2B1 isoforms enable the highly specialized fine-tuning between neurite outgrowth versus retraction that is required for the formation and maintenance of the neuronal synapses that are needed to properly regulate energy balance. Cells in nonbrain tissues may not have a need for such specialized fine-tuning, perhaps explaining why the α isoform evolved almost exclusively in the brain. Indeed, in a variety of assays in other nonbrain cell types, in response to a variety of ligands, SH2B1α functions similarly to SH2B1β/γ (1,40,41). Whether SH2B1δ also has unique functions relevant to the brain is not yet known. Unfortunately, it was not possible to parse the individual contributions of SH2B1α or SH2B1δ by deleting either isoform individually because of the *Sh2b1* gene structure. However, based on protein levels of SH2B1 detected by Western blotting, the α isoform is present at much higher levels than the δ isoform, suggesting that removal of the α isoform may make the major contribution to the αδKO phenotype.

Which brain cells might be driving the αδKO phenotype? Despite prior evidence suggesting that SH2B1 contributes to energy balance by modulating LepRb/JAK2 signaling (7), our data suggest that deletion of SH2B1α/δ does not alter cellular responses to leptin. Our RNA-seq data suggest that removal of SH2B1α/δ has the greatest impact on genes associated with cells of the immune system, including microglia. These are the first results to our knowledge that associate SH2B1 isoforms with microglial functions and, thus, highlight a novel focal point for follow-up studies. Microglia could contribute to the αδKO phenotype via complement-mediated synaptic pruning of appetite-regulating neuronal synapses. In fact, most of the microglia-related genes within our significantly differentially regulated gene set (*C1qa*, *C1qb*, *Cx3cr1*, *Grn*, *Trem2*, *Tyrobp*) have been identified as contributors to complement-mediated synaptic pruning (33–37). Whether the lack of SH2B1α/δ affects microglia function directly or indirectly, perhaps via neurons, remains to be determined.

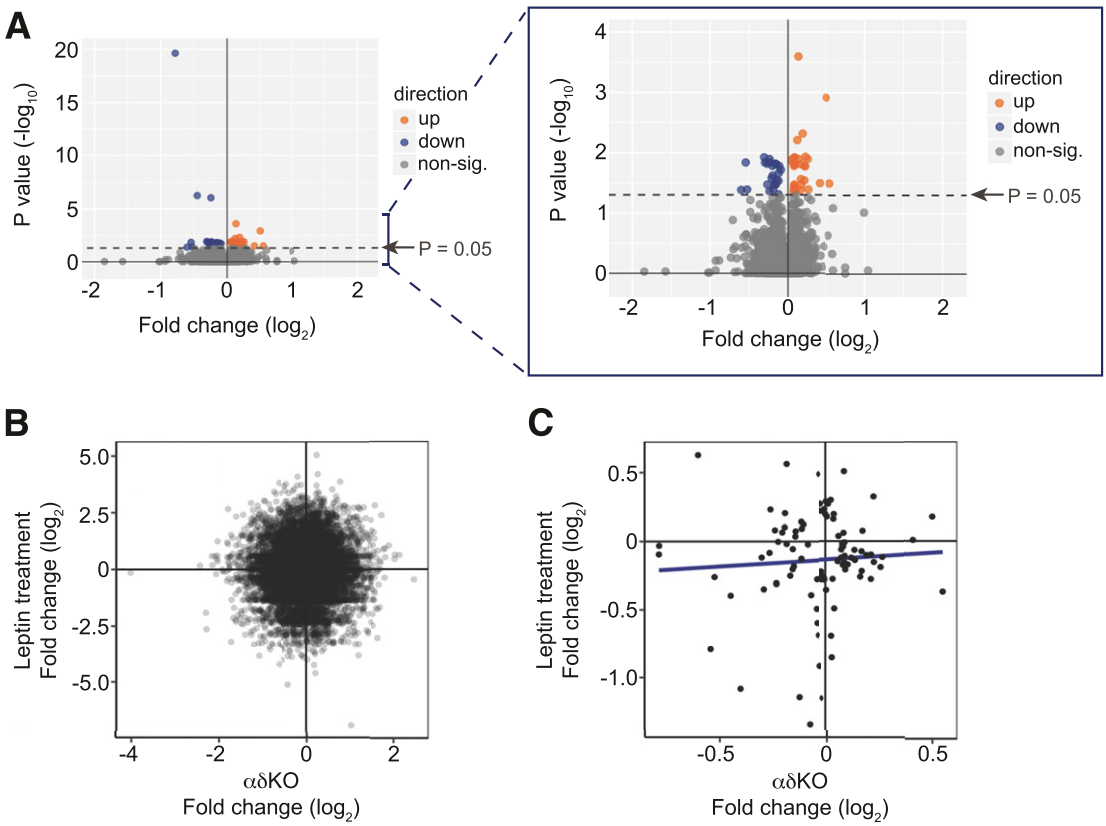

Figure 8—Altered transcriptome in αδKO mice. *A*: mRNA was isolated from hypothalami of 10- to 12-week-old male mice and analyzed by RNA-seq (*n*: WT = 9, αδKO = 12). Left: volcano plot depicts differentially expressed genes. Genes located above the dotted horizontal line are significantly ($P < 0.05$) upregulated (orange dots, $x > 0$) or significantly downregulated (dark-blue dots, $x < 0$) in αδKO mice. Genes located below the dotted line (gray dots) are not significantly regulated ($P \geq 0.05$). *Sh2b1* is not shown. Right: Enlargement of graph on left. non-sig., nonsignificant. *B*: Scatterplot compares differentially expressed genes from hypothalami of αδKO and leptin-treated mice ($r = 0.003$; $P = 0.616$). *C*: Scatterplot compares genes with statistically significant differential regulation between hypothalami of αδKO and leptin-treated mice ($r = 0.061$; $P = 0.56$). See Supplementary Figs. 4–6 for additional analyses of RNA-seq data. Statistics: see Supplementary Material.

Given the ability of SH2B1 to enhance signaling of neurotrophic factors and affect neuronal architecture, the αδKO phenotype could also be a consequence, at least in part, of altered neuronal activity. BDNF-sensitive neurons are attractive candidates for neurons affected in αδKO mice. BDNF and TrkB are critical regulators of metabolism (42). BDNF/TrkB activity is important for many neuronal processes that contribute to energy balance, including regulation of mature neural circuits through structural changes of dendritic spines at excitatory synapses. SH2B1β has been shown to enhance BDNF-induced neurite outgrowth of PC12 cells, regulate the actin cytoskeleton, and interact with actin-binding protein IRSp53 in primary cultured neurons to regulate the formation of dendritic filopodia—the small membranous protrusions that often develop into dendritic spines (10,11,13,14). Thus, SH2B1 isoforms could collectively fine-tune appetite-regulating neuronal synapses by mediating cytoskeletal rearrangement within dendritic spines of TrkB-expressing neurons, and perhaps the synaptic pruning carried out by microglia. In αδKO mice, we would predict that upregulated SH2B1β/γ activity would increase cytoskeletal rearrangement and thereby improve communication between appetite-regulating neurons to decrease appetite. Consistent with our hypothesis that activity downstream of TrkB is upregulated in αδKO hypothalami, administration of BDNF into various hypothalamic nuclei in mice reduces food intake and weight gain (43). Future experiments will be necessary to clarify whether TrkB or other receptor tyrosine kinases have altered activity in αδKO mice. Additional work will also be required to fully understand why the lean phenotype of αδKO mice appears to have arisen through distinct physiological mechanisms when mice were fed normal chow versus a HFD.

Alternative splicing generates much of the molecular and cellular diversity that exists, spatially and temporally, in the brain (44,45). However, alternative splicing is delicately regulated and has been shown to go awry. Indeed, prior studies have linked alternative splicing aberrations to neurological disorders (46) and metabolic dysregulation (47,48). Our work is unique in that it presents alternative

splicing not as a potential cause for disease but, rather, as an opportunity to treat disease. In other words, regardless of the exact cellular mechanisms involved, the bottom line of this report is that disrupting brain-specific alternative splicing of *Sh2b1* to delete SH2B1α/δ generates mice that are resistant to weight gain and seemingly healthy otherwise.

To summarize, our findings advance our understanding in four major ways. First, while removal of all SH2B1 isoforms induces obesity in mice (4), we show that deletion of the brain-specific SH2B1α/δ isoforms has the opposite effect, offering protection against obesity. Thus, for the first time, our data demonstrate unique, nonredundant functions of SH2B1 isoforms in vivo. Second, these results indicate that disrupting the alternative splicing of *Sh2b1* to delete the α and δ isoforms protects against weight gain, presenting a potential target for obesity therapeutics. Third, our research suggests that the α and δ isoforms of SH2B1 regulate energy homeostasis primarily via leptin-independent mechanisms. Fourth, our RNA-seq data set suggests potential cellular mechanisms by which isoforms of SH2B1 control energy balance—perhaps by refining synapses between appetite-regulating neurons in the hypothalamus. Together, these findings highlight the importance of alternative splicing in regulating brain function relevant to energy balance and illuminate several novel pathways that researchers might follow to gain more information about the mechanism(s) by which SH2B1 isoforms work together to regulate body weight.

Acknowledgments. The authors thank Dr. Ray Joe, Dr. Lei Yin, Dr. Xin (Tony) Tong, and Dr. Deqiang Zhang (University of Michigan) for feedback on experimental design and data analysis and Sarah Cain (University of Michigan) for administrative assistance. The authors thank Dr. Miriam Meisler, Dr. Carey Lumeng, and Dr. Malcolm Low (University of Michigan) for helpful discussions, Dr. Liangyou Rui (University of Michigan) for the gift of the *Sh2b1* KO strain, and Dr. Heimo Riedel (West Virginia University) for the cDNA encoding SH2B1γ. The authors acknowledge the Michigan Diabetes Research Center Molecular Genomics Core and Dr. Thomas Saunders, Galina Gavrilina, and Dr. Wanda Filipiak of the University of Michigan Transgenic Animal Model Core for help generating the αδKO mouse model.

Funding. This research was supported by National Institute of Diabetes and Digestive and Kidney Diseases, National Institutes of Health (NIH), grants R01-DK-054222 and R01-DK-107730 (to C.C.-S.), R01-DK-056731 (to M.G.M.), and R01-DK-062876 and R01-DK-092759 (to O.A.M.). J.L.C. was supported by a National Science Foundation Graduate Research Fellowship and a Rackham Predoctoral Fellowship from the Horace H. Rackham School of Graduate Studies at the University of Michigan. A.F. was supported by predoctoral fellowships from the Horace H. Rackham School of Graduate Studies at the University of Michigan (Rackham Merit Fellowship), the Systems and Integrative Biology Training Program (National Institute of General Medical Sciences, NIH, T32-GM-008322), and the Howard Hughes Medical Institute (Gilliam Fellowship for Advanced Study). L.C.D. was supported by an Endocrine Society Summer Research Fellowship and an American Physiological Society Undergraduate Summer Research Fellowship. D.P.B. was supported by predoctoral fellowships from the Medical Scientist Training Program (National Institute of General Medical Sciences, NIH, T32-GM-007863), Training Program for Organogenesis (National Institute of Child Health and Human Development, NIH, T32-HD-007605), and Horace H. Rackham School of Graduate Studies at the University of Michigan (Rackham Merit Fellowship). Mouse body composition and CLAMS studies were partially supported by the Michigan Diabetes Research Center (National Institute of Diabetes and Digestive and Kidney Diseases, NIH, P30-DK-020572), Michigan Nutrition Obesity Research Center (National Institute of Diabetes and Digestive and Kidney Diseases, NIH, P30-DK-089503), and Michigan Mouse Metabolic Phenotyping Center (National Institute of Diabetes and Digestive and Kidney Diseases, NIH, U2C-DK-110678). Generation of the CRISPR/Cas9 mice was partially supported by the Michigan Diabetes Research Center Molecular Genomics Core (NIH, P30-DK-020572). The authors thank MedImmune for the gift of recombinant mouse leptin.

Duality of Interest. D.P.B. was supported by a TYLENOL Future Care Scholarship. No other potential conflicts of interest relevant to this article were reported.

Author Contributions. J.L.C. directed and conducted experiments and prepared the manuscript including all figures. L.S.A. and A.F. designed and generated the αδKO mice. A.C.R. performed the initial bioinformatics analysis of RNA-seq data and generated plots for Fig. 8*B* and *C* and Supplementary Figs. 4*B–D*, 5*A*, and 6. J.M.C. performed qPCR assays (Figs. 1*C* and 7*A* and Supplementary Figs. 4*A* and 5*D*), ran Western blots (Fig. 1*G* and *H* and Supplementary Fig. 5*E*), and made the construct encoding GFP-SH2B18c (Supplementary Fig. 5*E*). L.C.D. and A.H.B. assisted with body weight and food intake studies, blood sample collections, harvests, and genotyping. D.P.B. prepared and imaged liver samples (Fig. 4*J*). P.B.V. performed neurite outgrowth experiments (Supplementary Fig. 5*F*). A.M.C. and E.S.C. assisted with genotyping and mouse colony maintenance. G.C. assisted with body weight studies and genotyping. All authors reviewed and approved the final content. J.L.C., L.S.A., O.A.M., M.G.M., and C.C.-S. developed the concepts and hypotheses, designed the experiments, and interpreted the data. L.S.A., O.A.M., M.G.M., and C.C.-S. made revisions to the manuscript. C.C.-S. is the guarantor of this work and, as such, had full access to all the data in the study and takes responsibility for the integrity of the data and the accuracy of the data analysis.

Prior Presentation. Parts of this work were presented in poster form or as short oral presentations at the Keystone Symposium: Neuronal Control of Appetite, Metabolism and Weight, Copenhagen, Denmark, 9–13 May 2017; the 48th Annual Scientific Meeting of the Michigan Chapter of the Society for Neuroscience, Ann Arbor, MI, 22 May 2017; the 2017 Gordon Research Conference on Neurotrophic Factors, Newport, RI, 4–9 June 2017; the Keystone Symposium: Functional Neurocircuitry of Feeding and Feeding Disorders, Banff, Alberta, Canada, 10–14 February 2019; ENDO 2019: the Endocrine Society Annual Meeting, New Orleans, LA, 23–26 March 2019; and the 2019 Gordon Research Conference on Neurotrophic Mechanisms in Health and Disease, Newport, RI, 2–7 June 2019.

References

1. Doche ME, Bochukova EG, Su HW, et al. Human SH2B1 mutations are associated with maladaptive behaviors and obesity [published correction appears in J Clin Invest 2013;123:526]. J Clin Invest 2012;122:4732–4736

2. Pearce LR, Joe R, Doche ME, et al. Functional characterisation of obesity-associated variants involving the alpha and beta isoforms of human SH2B1. Endocrinology 2014;155:3219–3226

3. Flores A, Argetsinger LS, Stadler LKJ, et al. Crucial role of the SH2B1 PH domain for the control of energy balance. Diabetes 2019;68:2049–2062

4. Ren D, Li M, Duan C, Rui L. Identification of SH2-B as a key regulator of leptin sensitivity, energy balance, and body weight in mice. Cell Metab 2005;2:95–104

5. Duan C, Yang H, White MF, Rui L. Disruption of the SH2-B gene causes age-dependent insulin resistance and glucose intolerance. Mol Cell Biol 2004;24:7435–7443

6. Ren D, Zhou Y, Morris D, Li M, Li Z, Rui L. Neuronal SH2B1 is essential for controlling energy and glucose homeostasis. J Clin Invest 2007;117:397–406

7. Rui L. SH2B1 regulation of energy balance, body weight, and glucose metabolism. World J Diabetes 2014;5:511–526

8. Emmerson PJ, Wang F, Du Y, et al. The metabolic effects of GDF15 are mediated by the orphan receptor GFRAL. Nat Med 2017;23:1215–1219

9. Chen L, Maures TJ, Jin H, et al. SH2B1β (SH2-Bβ) enhances expression of a subset of nerve growth factor-regulated genes important for neuronal differentiation including genes encoding uPAR and MMP3/10. Mol Endocrinol 2008;22:454–476
10. Diakonova M, Gunter DR, Herrington J, Carter-Su C. SH2-Bbeta is a Rac-binding protein that regulates cell motility. J Biol Chem 2002;277:10669–10677
11. Rider L, Tao J, Snyder S, Brinley B, Lu J, Diakonova M. Adapter protein SH2B1β cross-links actin filaments and regulates actin cytoskeleton. Mol Endocrinol 2009;23:1065–1076
12. Zhang Y, Zhu W, Wang YG, et al. Interaction of SH2-Bbeta with RET is involved in signaling of GDNF-induced neurite outgrowth. J Cell Sci 2006;119:1666–1676
13. Shih CH, Chen CJ, Chen L. New function of the adaptor protein SH2B1 in brain-derived neurotrophic factor-induced neurite outgrowth. PLoS One 2013;8:e79619
14. Chen CJ, Shih CH, Chang YJ, et al. SH2B1 and IRSp53 proteins promote the formation of dendrites and dendritic branches. J Biol Chem 2015;290:6010–6021
15. Rui L, Herrington J, Carter-Su C. SH2-B is required for nerve growth factor-induced neuronal differentiation. J Biol Chem 1999;274:10590–10594
16. Qian X, Riccio A, Zhang Y, Ginty DD. Identification and characterization of novel substrates of Trk receptors in developing neurons. Neuron 1998;21:1017–1029
17. Myers MG, Leibel RL. Lessons from rodent models of obesity. In *Endotext*. Feingold KR, Anawalt B, Boyce A,et al, Eds. South Dartmouth, MA, MDText.com, Inc, 2000
18. Joe RM, Flores A, Doche ME, et al. Phosphorylation of the unique C-terminal tail of the alpha isoform of the scaffold protein SH2B1 controls the ability of SH2B1α to enhance nerve growth factor function. Mol Cell Biol 2018;38:e00277-17
19. Ran FA, Hsu PD, Wright J, Agarwala V, Scott DA, Zhang F. Genome engineering using the CRISPR-Cas9 system. Nat Protoc 2013;8:2281–2308
20. Parlee SD, Lentz SI, Mori H, MacDougald OA. Quantifying size and number of adipocytes in adipose tissue. Methods Enzymol 2014;537:93–122
21. Mina AI, LeClair RA, LeClair KB, Cohen DE, Lantier L, Banks AS. CalR: a web-based analysis tool for indirect calorimetry experiments. Cell Metab 2018;28:656–666.e1
22. Nelms K, O'Neill TJ, Li S, Hubbard SR, Gustafson TA, Paul WE. Alternative splicing, gene localization, and binding of SH2-B to the insulin receptor kinase domain. Mamm Genome 1999;10:1160–1167
23. Yousaf N, Deng Y, Kang Y, Riedel H. Four PSM/SH2-B alternative splice variants and their differential roles in mitogenesis. J Biol Chem 2001;276:40940–40948
24. Tortoriello DV, McMinn J, Chua SC. Dietary-induced obesity and hypothalamic infertility in female DBA/2J mice. Endocrinology 2004;145:1238–1247
25. Yang Y, Smith DL Jr., Keating KD, Allison DB, Nagy TR. Variations in body weight, food intake and body composition after long-term high-fat diet feeding in C57BL/6J mice. Obesity (Silver Spring) 2014;22:2147–2155
26. Patterson CM, Leshan RL, Jones JC, Myers MG Jr. Molecular mapping of mouse brain regions innervated by leptin receptor-expressing cells. Brain Res 2011;1378:18–28
27. Scott MM, Lachey JL, Sternson SM, et al. Leptin targets in the mouse brain. J Comp Neurol 2009;514:518–532
28. Flak JN, Myers MG Jr. Minireview: CNS mechanisms of leptin action. Mol Endocrinol 2016;30:3–12
29. Allison MB, Pan W, MacKenzie A, et al. Defining the transcriptional targets of leptin reveals a role for *Atf3* in leptin action. Diabetes 2018;67:1093–1104
30. Björnholm M, Münzberg H, Leshan RL, et al. Mice lacking inhibitory leptin receptor signals are lean with normal endocrine function. J Clin Invest 2007;117:1354–1360
31. Rupp AC, Allison MB, Jones JC, et al. Specific subpopulations of hypothalamic leptin receptor-expressing neurons mediate the effects of early developmental leptin receptor deletion on energy balance. Mol Metab 2018;14:130–138
32. Chen R, Wu X, Jiang L, Zhang Y. Single-cell RNA-seq reveals hypothalamic cell diversity. Cell Rep 2017;18:3227–3241
33. Filipello F, Morini R, Corradini I, et al. The microglial innate immune receptor TREM2 is required for synapse elimination and normal brain connectivity. Immunity 2018;48:979–991.e8
34. Hoshiko M, Arnoux I, Avignone E, Yamamoto N, Audinat E. Deficiency of the microglial receptor CX3CR1 impairs postnatal functional development of thalamocortical synapses in the barrel cortex. J Neurosci 2012;32:15106–15111
35. Paolicelli RC, Bolasco G, Pagani F, et al. Synaptic pruning by microglia is necessary for normal brain development. Science 2011;333:1456–1458
36. Zhang B, Gaiteri C, Bodea LG, et al. Integrated systems approach identifies genetic nodes and networks in late-onset Alzheimer's disease. Cell 2013;153:707–720
37. Stevens B, Allen NJ, Vazquez LE, et al. The classical complement cascade mediates CNS synapse elimination. Cell 2007;131:1164–1178
38. Popp MW, Maquat LE. Leveraging rules of nonsense-mediated mRNA decay for genome engineering and personalized medicine. Cell 2016;165:1319–1322
39. Möröy T, Heyd F. The impact of alternative splicing in vivo: mouse models show the way. RNA 2007;13:1155–1171
40. Zhang M, Deng Y, Riedel H. PSM/SH2B1 splice variants: critical role in src catalytic activation and the resulting STAT3s-mediated mitogenic response. J Cell Biochem 2008;104:105–118
41. Zhang M, Deng Y, Tandon R, Bai C, Riedel H. Essential role of PSM/SH2-B variants in insulin receptor catalytic activation and the resulting cellular responses. J Cell Biochem 2008;103:162–181
42. Rios M. BDNF and the central control of feeding: accidental bystander or essential player? Trends Neurosci 2013;36:83–90
43. Noble EE, Billington CJ, Kotz CM, Wang C. The lighter side of BDNF. Am J Physiol Regul Integr Comp Physiol 2011;300:R1053–R1069
44. Lipscombe D. Neuronal proteins custom designed by alternative splicing. Curr Opin Neurobiol 2005;15:358–363
45. Li Q, Lee JA, Black DL. Neuronal regulation of alternative pre-mRNA splicing. Nat Rev Neurosci 2007;8:819–831
46. Licatalosi DD, Darnell RB. Splicing regulation in neurologic disease. Neuron 2006;52:93–101
47. Kaminska D, Pihlajamäki J. Regulation of alternative splicing in obesity and weight loss. Adipocyte 2013;2:143–147
48. Wong CM, Xu L, Yau MY. Alternative mRNA splicing in the pathogenesis of obesity. Int J Mol Sci 2018;19:632